



# Improvement of cycle property of sulfur-coated multi-walled carbon nanotubes composite cathode for lithium/sulfur batteries

Lixia Yuan, Huiping Yuan, Xinping Qiu\*, Liquan Chen, Wentao Zhu

Key Laboratory of Organic Optoelectronics and Molecular Engineering, Department of Chemistry, Tsinghua University, Beijing 100084, China

## ARTICLE INFO

### Article history:

Received 22 August 2008  
Received in revised form 24 December 2008  
Accepted 29 December 2008  
Available online 17 January 2009

### Keywords:

Multi-walled carbon nanotubes  
Capillarity  
Lithium/sulfur batteries  
Cycle property  
Well-distributed morphology

## ABSTRACT

A novel sulfur-coated multi-walled carbon nanotubes composite material (S-coated-MWCNTs) was prepared through capillarity between the sulfur and multi-walled carbon nanotubes. The results of the TEM and XRD measurements reveal that S-coated-MWCNTs have a typical core-shell structure, and the MWCNTs serve as the cores and are dispersed individually into the sulfur matrices. The charge–discharge experiments of the lithium/sulfur cells demonstrated that the S-coated-MWCNTs cathode could maintain a reversible capacity of  $670 \text{ mAh g}^{-1}$  after 60 cycles, showing a greatly enhanced cycle ability as compared with the sulfur cathode with simple MWCNTs addition (S/MWCNTs) and the cathode using sulfur-coated carbon black composite (S-coated-CB). The EIS and SEM techniques were used to define and understand the impact of the microstructure of the composite electrode on its electrochemical performance. Derived from these studies, the main key factors to the improvement in the cycle life of the sulfur cathode were discussed.

© 2009 Published by Elsevier B.V.

## 1. Introduction

Development of high energy density rechargeable batteries is becoming more and more important because of the increasing energy consumption of portable and transport applications [1]. For all the redox couples enabling for rechargeable batteries, lithium/sulfur couple has almost the highest specific-energy of  $2600 \text{ Wh kg}^{-1}$  [2,3], because the theoretical capacity of sulfur is highest ( $1672 \text{ mAh g}^{-1}$ ) among all the possible solid compounds known for primary and rechargeable cathodes. In addition to the high capacity, elemental sulfur also has advantages of natural abundance, low cost and low toxicity, which are all the important factors for next generation of lithium batteries.

However, the realization of lithium/sulfur battery has a number of difficult problems to overcome. Typically, the biggest shortfall exhibited with these systems is a difficulty to sustain long cycle life. Previous cyclic voltammetry and ultraviolet analyses suggest that the discharge reaction of sulfur always consists of stepwise reduction processes and generates various forms of intermediate polysulfides which can dissolve in the electrolyte specially selected for lithium/sulfur batteries [4–6]. Because the redox reaction of sulfur cathode can only occur at the surface of carbon for the insulating nature of sulfur and its reduction products [7], the facile transport of the polysulfides to carbon matrix is very important for a high sulfur utilization. Furthermore, the electrochemical reduction

of sulfur cathode is a complicate process composed of a series of electron transfer reactions, coupled with the phase transition of the sulfur species, so the structure of the sulfur electrode would be unavoidably changed during the discharge–charge cycles [8–10]. It was found that the sulfur composite electrodes expanded when discharging and shrank when charging again and the thickness change of the electrode was measured to be about 22% [11]. Cheon et al. also indicated that the capacity fading in a high-energy-density sulfur cathode is mainly due to the structural failure by physical crack propagations of the electrode structure and subsequent formation of the electrochemically irreversible  $\text{Li}_2\text{S}$  layer at cracked surfaces of carbon particles or masses [12]. Therefore, for a high performance sulfur cathode, it is not trivial to control the morphology of the cathode such as the carbon matrix's uniformity and structural stability. Recently, Han et al. reported that the use of multi-walled carbon nanotubes (MWCNTs) instead of acetylene black in the cathode can increase not only rate capability but also the cycle life of the sulfur electrode [13]. MWCNTs should be an attractive choice as the electric conductor for sulfur cathode because they can provide a more effective electronically conductive network than the traditional conductive additives, such as carbon black (CB) and acetylene black (AB). While the MWCNTs have a drawback to overcome that they are difficult to be dispersed into sulfur electrode homogeneously [14], which leads that the cycle performance of a sulfur cathode with simple MCNTs addition still remains insufficient for practical application.

In this work, we designed and prepared sulfur-coated multi-walled carbon nanotubes composite material (S-coated-MWCNTs), and tried to use this one-dimension nanosized material to develop a

\* Corresponding author. Tel.: +86 10 62794234; fax: +86 10 62794234.  
E-mail address: [qixp@tsinghua.edu.cn](mailto:qixp@tsinghua.edu.cn) (X. Qiu).

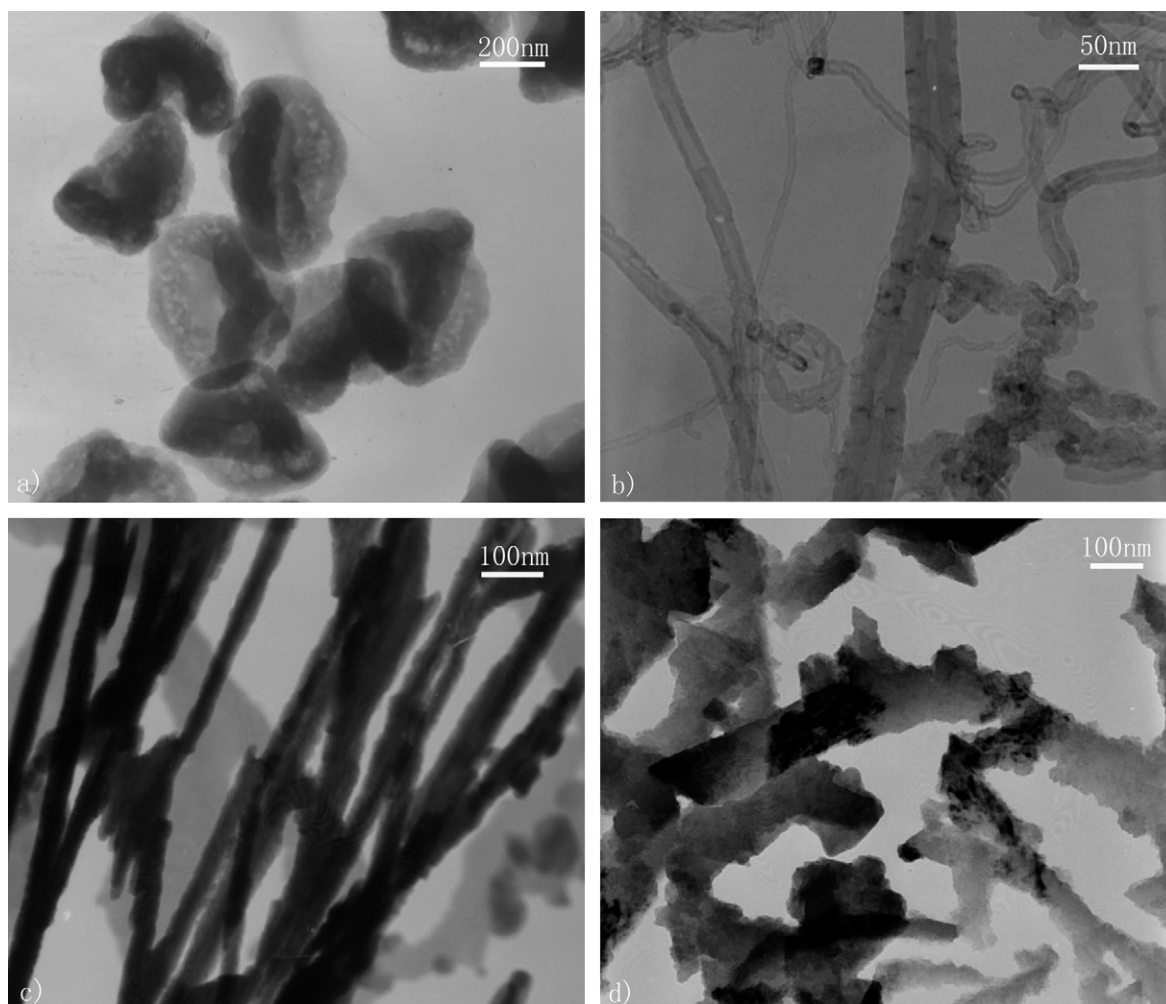


Fig. 1. TEM images of (a) elemental sulfur, (b) MWCNTs, (c) S-coated-MWCNTs (50% sulfur) and (d) S-coated-MWCNTs (80% sulfur).

dense sulfur cathode with well-distributed morphology to accommodate the mechanical stress induced by volume change caused by redox reaction of sulfur during the charge–discharge cycles. The electrochemical performance of the composite cathode was investigated in detail. The other two types of sulfur cathodes: a sulfur cathode with simple MWCNTs addition (S/MWCNTs) and another cathode using sulfur-coated carbon black composite (S-coated-CB) were also fabricated for the purpose of comparison.

## 2. Experimental

### 2.1. Preparation of materials

The S-coated-MWCNTs were prepared through capillarity between sulfur and MWCNTs because sulfur is a substance with low surface tension of  $61 \text{ mN m}^{-1}$  and can wet and fill carbon nanotubes through capillarity [15]. In order to purify the MWCNTs, the raw MWCNTs (95% purity, 20–50 nm, Beijing, China) were soaked in nitric acid at  $80^\circ\text{C}$  for 4 h and then washed by distilled water until pH value of the filtrate reached 7.0. A typical procedure for preparing S-coated-MWCNTs was first to mix the elemental sulfur (Analytical grade, Shanghai, China) and MWCNTs by mechanical ball milling for 5 h, then to sealed the mixture in a PTFE container filled with argon gas, and finally to place the container in an oven at  $155^\circ\text{C}$  for 24 h.

### 2.2. Preparation of the sulfur cathodes

All the cathodes were prepared by mixing 85 wt.% sulfur composite powder, 5 wt.% carbon black and 10 wt.% polytetrafluoroethylene (PTFE, in diluted emulsion) with 2-propanol to form a paste, and then roll-pressing the paste into ca. 0.1 mm thick film and finally pressing the film onto a nickel net.

### 2.3. Electrochemical measurements

The testing cells had a typical three-electrode construction using lithium foils as both the counter and reference electrodes, Cellgard 2400 microporous membrane as separator and 1.0 M  $\text{LiN}(\text{CF}_3\text{SO}_2)_2$  dissolved in dimethoxyethane (DME) and dioxolane (DOL) (1:1, v/v) as the electrolyte. The cells were assembled in an argon-filled glove box. The discharge–charge tests were carried out with a BTS-5 V/5 mA type battery charger (Shenzhen, China) at a current density of  $100 \text{ mA g}^{-1}$ -sulfur in the voltage range 1.5–2.5 V vs.  $\text{Li/Li}^+$ . EIS measurements were performed using Solartron FRA 1255B frequency response analyzer in combination with the potentiostat. The impedance diagrams were plotted at the open circuit voltages (OCVs) from the original batteries and the full charged batteries after 40 cycles. For the latter, a constant voltage (2.5 V vs.  $\text{Li/Li}^+$ ) was first applied by the potentiostat until the equilibrium state was reached, characterized by a zero current value. Then, the EIS measurements were carried out in a frequency range between 100 kHz

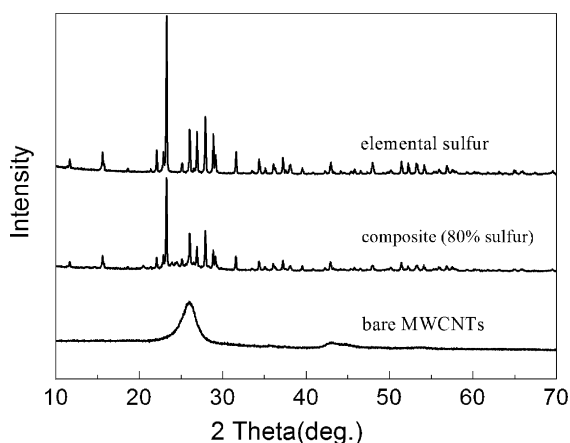


Fig. 2. X-ray diffraction patterns of the S-coated-MWCNTs (80% sulfur).

and 100 mHz at potentiostatic signal amplitudes of 5 mV. All experiments were conducted at room temperature.

#### 2.4. Structural characterization

The morphology of S-coated-MWCNTs was investigated using transmission electron microscopy (TEM, JEM-1200EX) operated at 200 keV. The XRD patterns of the as-prepared products were investigated via a Bruker powder diffraction system (model D8 Advanced), using Cu K $\alpha$  as the radiation source at the operating voltage of 40 kV and a scan rate of 6° min<sup>-1</sup>.

The changes in the surface morphology of the sulfur cathodes during discharge–charge cycles were examined by scanning electron microscopy (SEM) on a JSM-6301F system (Japan). Before SEM measurements, the remaining soluble polysulfide in the cathode was completely washed with DME. Therefore, only solid compounds were observed in the SEM images.

### 3. Results and discussion

#### 3.1. The structure characterization

Fig. 1 shows the morphological characterizations of elemental sulfur, MWCNTs and their composites prepared through capillarity. The diameter of the sulfur-coated-MWCNTs become larger than that of the original MWCNTs before coating treatment. Clearly, a tubular layer of a continuously and uniformly coated sulfur film is present on the MWCNT surface. The S-coated-MWCNTs should have

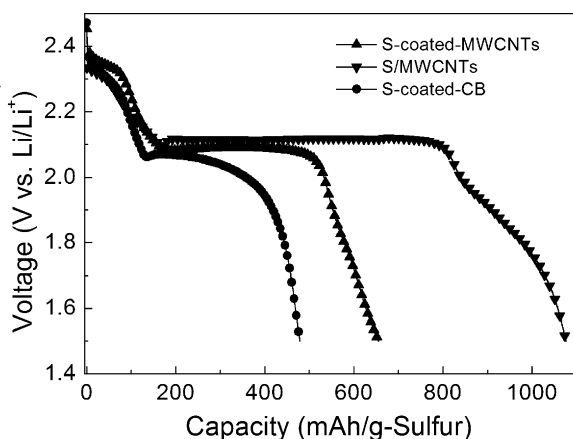


Fig. 3. Initial discharge curves of lithium/sulfur batteries at a current of 100 mA g<sup>-1</sup>-sulfur.

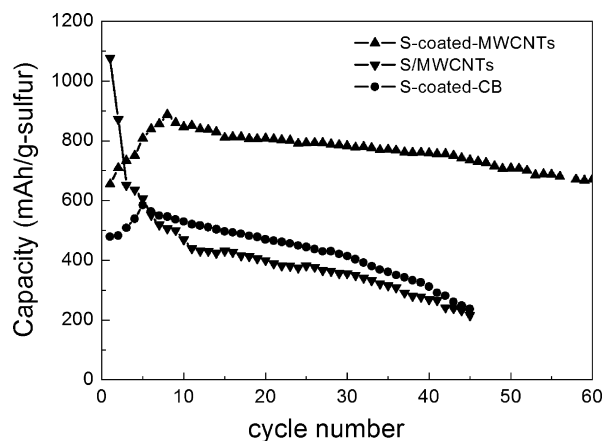


Fig. 4. A comparison of the cycling performances of S-coated-MWCNTs and S-coated-CB cathodes in the range of 2.5–1.5 V vs. Li/Li<sup>+</sup> at a current of 100 mA g<sup>-1</sup>-sulfur.

a typical core-shell structure, and the MWCNTs serve as the cores and are dispersed individually into the sulfur matrices. Furthermore, the average thickness of the sulfur layer ranges from several to tens of nanometers, depending on the sulfur content (Fig. 1c and d). When the composite contains 80% sulfur, its shell thickness is about 30 nm.

To further confirm the nanostructure of the S-coated-MWCNTs, the XRD patterns are given in Fig. 2. The reflections of the raw sulfur are consistent with Fddd orthorhombic structure. Compared

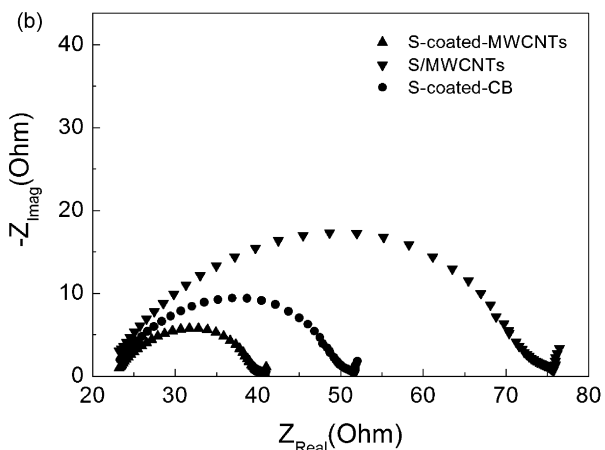
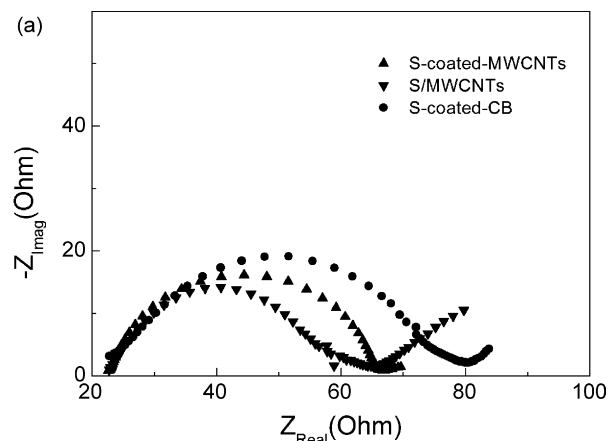
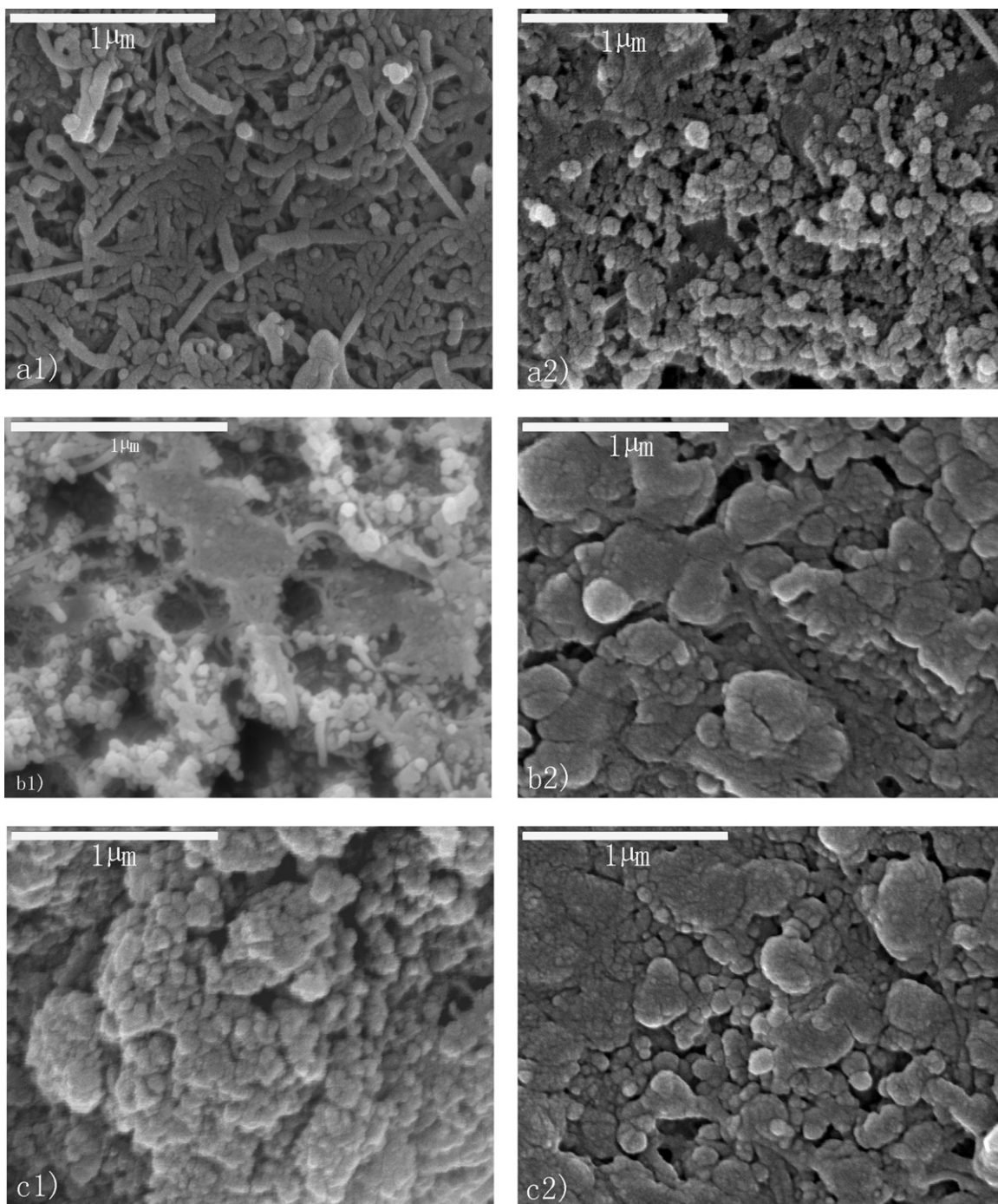


Fig. 5. Nyquist plots for sulfur cathodes in the frequency range of (100 kHz to 100 mHz): (a) before discharge and (b) after 40 cycles.





**Fig. 6.** SEM images of the sulfur cathodes. (a1) and (a2): S-coated-MWCNTs cathode, original and after 40 cycles; (b1) and (b2): S/MWCNTs cathode, original and after 40 cycles; (c1) and (c2): S-coated-CB cathode, original and after 40 cycles.

with the pattern of the raw elemental sulfur, the XRD spectra of the S-coated-MWCNTs did not exhibit many changes except for the appearance of the slight and broad MWCNTs peaks centered at  $2\theta = 26^\circ$ , indicating that no phase transformation occurred during capillarity treatment and the crystal structure of sulfur still remains orthorhombic structure.

### 3.2. Electrochemical performance of the S-coated-MWCNTs

In order to investigate the effect of MWCNTs on the electrochemical performance of the sulfur cathode, three types of sulfur composites were used to fabricate cathodes. One was sulfur-coated MWCNTs composite mentioned above (S-coated-MWCNTs);

another was sulfur/MWCNTs composite prepared by simply ball milling (S/MWCNTs); the third was sulfur-coated carbon black composite (S-coated-CB) prepared by the same way as S-coated-MWCNTs. All cathodes comprise the same proportion of elemental sulfur (68%). Fig. 3 depicts the first discharge curves of the three types of sulfur electrodes measured in half-cells. All the discharge curves show two plateaus based on the voltage profile. The detailed mechanisms for oxidation and reduction of sulfur, polysulfides and lithium sulfide during discharge-charge were already reported [4–6]. The upper plateau is well known as the change from elemental sulfur to the higher order lithium polysulfides ( $\text{Li}_2\text{S}_n$ ,  $n \geq 4$ ). The lower plateau is caused by the reduction of the higher order lithium polysulfides to lower order lithium polysulfides ( $\text{Li}_2\text{S}_n$ ,

$n < 4$ ), even to  $\text{Li}_2\text{S}$ . Theoretically, standard potentials of the upper and lower plateau are 2.33 V and 2.18 V vs.  $\text{Li}/\text{Li}^+$ , respectively. While, some degrees of discharge voltage drop always take place in practical cell systems. This voltage drop should be contributed to IR loss, which is mainly generated by the internal resistance of the cell. Here, internal resistance consists of ionic resistance of the electrolyte, electronic resistance of electrode–current collector and interfacial resistance between electrode and electrolyte. In case of the S-coated-MWCNTs cathode and the S-coated-CB cathode, a little more voltage drop occurred than S/MWCNTs cathode. This could be explained by the core-shell structure of these two composites and the high conducting carbon materials was coated by the insulating sulfur. Furthermore, these two composite cathodes also show lower initial discharge capacity of  $655 \text{ mAh g}^{-1}$  (S-coated-MWCNTs) and  $480 \text{ mAh g}^{-1}$  (S-coated-CB), respectively, contrasting to the  $1075 \text{ mAh g}^{-1}$  of S/MWCNTs cathode. However, S-coated-MWCNTs cathode shows an outstanding cycle performance. Fig. 4 shows the cycle life pattern of S-coated MWCNTs cathode and the data from S/MWCNTs and S-coated-CB cathodes at the same experimental conditions are also shown for comparison. In the case of S/MWCNTs cathode, it is clearly seen that the discharge capacity decreased drastically with increasing cycle number. Only after 40 cycles, most of its initial discharge capacity is lost and saturated to  $270 \text{ mAh g}^{-1}$ . It is typical cyclic behavior of lithium/sulfur battery with liquid type electrolyte. On the contrary, the cycle life of S-coated-MWCNTs cathode was greatly improved and gave a reversible capacity of  $670 \text{ mAh g}^{-1}$  after 60 cycles. As shown in Fig. 4, the reversible capacity of S-coated-MWCNTs cathode shows a gradual increase during the first 8 cycles. This could also be explained by its core-shell structure that the high conducting carbon materials was coated by the insulating sulfur while the redox reaction of sulfur cathode can only occur at the surface of carbon. During the first several cycles, the surface of the MWCNTs uncovered to the electrolyte gradually increased with the phase change of sulfur from a solid state to the dissolved polysulfide state. These results were consistent with the lower initial discharge capacity. The improvement of the cycle life may be contributed to the good electrical path and structural stability given by well-distributed carbon nanotubes in the S-coated-MWCNTs cathode. Cycle life improved substantially when the uniformity of MWCNTs distribution in the sulfur cathode improved. In addition, the S-coated-MWCNTs cathode shows a better cycle performance than the S-coated-CB cathode, which should be owed to the one-dimension nanosized structure of the MWCNTs which is beneficial to construct a sturdier three-dimensional carbon network matrix to accommodate the mechanical stress induced by volume change caused by the redox reaction of sulfur during the discharge–charge cycles.

Fig. 5 shows typical Nyquist plots of sulfur cathodes before discharge and after 40 cycles. It can be seen from the figures that all the Nyquist plots of sulfur cathodes are composed by a semicircle at high frequencies corresponding to the contact resistance and charge transfer resistance and a short inclined line in low frequency regions due to the ion diffusion within the cathode. Before discharge, the S-coated-MWCNTs cathode and S-coated-CB cathode show higher charge-transfer resistances ( $R_{ct}$ ) than S/MWCNTs cathode (Fig. 5a). While after the first 40 cycles, the charge-transfer resistances of S-coated-MWCNTs cathode and S-coated-CB cathode decrease from  $43 \Omega$  and  $56 \Omega$  to  $16 \Omega$  and  $28 \Omega$ , respectively, which should be contributed to that the surface of the MWCNTs and CB uncovered to the electrolyte gradually increased with the phase change of sulfur from a solid state to the dissolved polysulfide state. It is corresponding to the increase of the reversible capacity in the first several cycles. As for the increases in the  $R_{ct}$  of the S/MWCNTs cathode, the main reason may be the poor electrical contact originated by severe morphology change of sulfur cathode. Comparing

the EIS change of these three types of cathodes, two conclusions can be drawn: one is that MWCNTs can provide a more effective electronically conductive network than the traditional electric conductor. The other is that the electrochemical performance of the sulfur cathode is affected significantly by the quality of the sulfur and the electric conductor dispersion within the electrode.

### 3.3. Morphological changes of the cathodes

The conclusions mentioned above also can be confirmed by the results of the SEM analysis. Fig. 6 shows the SEM images of the three types of cathode at different cycles. It is seen in Fig. 6a1 that in the original S-coated-MWCNTs cathode, S-coated-MWCNTs are well-distributed as individual tubes and the core-shell structure of the composites ensures the contact area between the sulfur and MWCNTs. While in the original S/MWCNTs cathode, the sulfur particles agglomerate and the MWCNTs disperse as bundles as shown in Fig. 6b1. After 40 cycles, the S-coated-MWCNTs cathode still displays a homogeneous distribution of the cathode materials as shown in Fig. 6a2. However, agglomeration of sulfur or lithium sulfide of the S/MWCNTs cathode as shown in Fig. 6b2 became severe, which may be the main reason for the poor cyclic durability of the S/MWCNTs cathode. As to the S-coated-CB cathode, although a well-distributed morphology was observed before discharge as shown in Fig. 6c1, aggregation of sulfur or lithium sulfide also displayed after 40 cycles. The results of the SEM analysis seem to suggest that the capacity fading for the composite sulfur cathodes is mainly due to the heterogeneity of the cathode's morphology, which could worsen the distribution of sulfur or lithium sulfide along with cycling, and a sulfur cathode with well dispersed MWCNTs can suppress the agglomeration of sulfur or lithium sulfide which may be contributed to the electrical path provided by network-like structure constructed by the MWCNTs. These results are in good agreement with the results from the electrochemical measurement.

## 4. Conclusion

A novel sulfur-coated multi-walled carbon nanotubes composite material (S-coated-MWCNTs) was prepared through capillarity between the sulfur and multi-walled carbon nanotubes. The charge–discharge experiments demonstrated that the S-coated-MWCNTs cathode could maintain a reversible capacity of  $670 \text{ mAh g}^{-1}$  after 60 cycles, showing a greatly improved cycle property as compared with the sulfur cathode with simple MWCNTs addition (S/MWCNTs) and the cathode using sulfur-coated carbon black composite (S-coated-CB). The improvement of cycle property of S-coated-MWCNTs cathode was suggested to arise from not only the introduction of the MWCNTs, but also the homogeneous distribution of the MWCNTs in the composite cathode, which help to stabilize the structure of the sulfur cathode during discharge–charge cycles.

## Acknowledgements

The authors gratefully acknowledge the financial support by the National Natural Science Foundation of China (20803042) and the National 973 Program, China (Grant No. 2009CB220105).

## References

- [1] A.G. Ritchie, J. Power Sources 136 (2004) 285.
- [2] N. Petr, M. Klaus, K.S.V. Santhanam, H. Otto, Chem. Rev. 97 (1997) 207.
- [3] M.Y. Chu, US Patent 5,814,420 (1998).
- [4] H. Yamin, A. Gorenshtein, J. Penciner, Y. Sternberg, E. Peled, J. Electrochem. Soc. 135 (1988) 1045.

- [5] D. Marmorstein, T.H. Yu, K.A. Striebel, F.R. McLarnon, J. Hou, E.J. Cairns, J. Power Sources 89 (2000) 219.
- [6] D.H. Han, B.S. Kim, S.J. Choi, Y. Jung, J. Kwak, S.M. Park, J. Electrochem. Soc. 151 (9) (2004) E283.
- [7] J.A. Dean (Ed.), Lange's Handbook of Chemistry, third ed., McGraw-Hill, New York, 1985, pp. 3–5.
- [8] S.E. Cheon, K.S. Ko, J.H. Cho, S.W. Kim, E.Y. Chin, H.T. Kim, J. Electrochem. Soc. 150 (2003) A800.
- [9] S.E. Cheon, K.S. Ko, J.H. Cho, S.W. Kim, E.Y. Chin, H.T. Kim, J. Electrochem. Soc. 150 (2003) A796.
- [10] H.S. Ryua, H.J. Ahna, K.W. Kima, J.H. Ahn, J.Y. Lee, J. Power Sources 153 (2006) 360.
- [11] X. He, J. Ren, L. Wang, W. Pu, C. Jiang, C. Wan, J. Power Sources (2008), doi:10.1016/j.jpowsour.2008.07.034.
- [12] S.E. Cheon, S.S. Choi, J.S. Han, Y.S. Choi, B.H. Jung, H.S. Lim, J. Electrochem. Soc. 151 (12) (2004) A2067.
- [13] S.C. Han, M.S. Song, H. Lee, H.S. Kim, H.J. Ahn, J.Y. Lee, J. Electrochem. Soc. 150 (7) (2003) A889.
- [14] Y.J. Choi, K.W. Kim, H.J. Ahn, J.H. Ahn, J. Alloys Compd. 449 (2008) 313.
- [15] E. Dujardine, T.W. Ebbesen, H. Hiura, K. Tanigaki, Science 265 (1994) 1850.